# High-frequency guided ultrasonic waves to monitor corrosion thickness loss

Paul Fromme, Fabian Bernhard, and Bernard Masserey

Citation: AIP Conference Proceedings **1806**, 030006 (2017); doi: 10.1063/1.4974574
View online: https://doi.org/10.1063/1.4974574
View Table of Contents: http://aip.scitation.org/toc/apc/1806/1
Published by the American Institute of Physics

# High-Frequency Guided Ultrasonic Waves to Monitor Corrosion Thickness Loss

Paul Fromme[1,a], Fabian Bernhard[2], and Bernard Masserey[2]

[1] Department of Mechanical Engineering, University College London, WC1E 7JE, UK
[2] Department of Mechanical Engineering, University of Applied Sciences, Fribourg, Switzerland

a)p.fromme@ucl.ac.uk

**Abstract.** Corrosion due to adverse environmental conditions can occur for a range of industrial structures, e.g., ships and offshore oil platforms. Pitting corrosion and generalized corrosion can lead to the reduction of the strength and thus degradation of the structural integrity. The nondestructive detection and monitoring of corrosion damage in difficult to access areas can be achieved using high frequency guided ultrasonic waves propagating along the structure. Using standard ultrasonic transducers with single sided access to the structure, the two fundamental Lamb wave modes were selectively generated simultaneously, penetrating through the complete thickness of the structure. The wave propagation and interference of the guided wave modes depends on the thickness of the structure. Numerical simulations were performed using a 2D Finite Difference Method (FDM) algorithm in order to visualize the guided wave propagation and energy transfer across the plate thickness. Laboratory experiments were conducted and the wall thickness reduced initially uniformly by milling of the steel structure. Further measurements were conducted using accelerated corrosion in salt water. From the measured signal change due to the wave mode interference, the wall thickness reduction was monitored and good agreement with theoretical predictions was achieved. Corrosion can lead to non-uniform thickness reduction and the influence of this on the propagation of the high frequency guided ultrasonic waves was investigated. The wave propagation in a steel specimen with varying thickness was measured experimentally and the influence on the wave propagation characteristics quantified.

## INTRODUCTION

Corrosion leading to wall thickness loss is an important factor for marine structures, e.g., ships and offshore platforms. Generalized corrosion prevalent in ship hulls leads to thickness reduction, limiting their remaining service life [1]. Ship hulls, offshore oil platforms and oil storage tanks are built using large plate components. Nondestructive measurements of such structures can help to quantify the corrosion damage severity and to predict and hence prevent failure [2]. Ultrasonic measurements have good sensitivity to small thickness changes. Efficient monitoring of the structural integrity of large areas of industrial structures can be achieved using guided ultrasonic wave array systems [3-5]. Guided ultrasonic waves can propagate over large distances in thin structures [6, 7]. This allows for the nondestructive testing and monitoring of large technical structures [8]. Guided wave monitoring systems usually operate at low frequencies below the cut-off frequencies for higher order wave modes to selectively generate only the fundamental ($A_0$ or $S_0$) wave modes (Fig. 1), simplifying signal interpretation [9, 10]. The low operating frequency range leads to long wavelengths and thus limited sensitivity for the detection of small defects. The application of guided ultrasonic wave modes in the higher frequency-thickness range has been investigated to obtain better sensitivity for small defects. The $S_0$ mode (around 5 MHz mm) was used for corrosion detection in aircraft structures [11], and longitudinal modes (above 15 MHz mm) were employed for plate inspection [12]. Higher order mode clusters of guided wave modes up to about 20 MHz mm were used to monitor plates [13]. High frequency guided waves (coupled $A_0$ and $S_0$ modes) at around 6-7 MHz mm have been employed for the detection and localization of surface defects in plates [14], inspection of ribbed structures [15], fatigue crack monitoring in single [16] and multi-layer [17, 18] aluminum aerospace components.

*43rd Annual Review of Progress in Quantitative Nondestructive Evaluation, Volume 36*
AIP Conf. Proc. 1806, 030006-1–030006-8; doi: 10.1063/1.4974574
Published by AIP Publishing. 978-0-7354-1474-7/$30.00

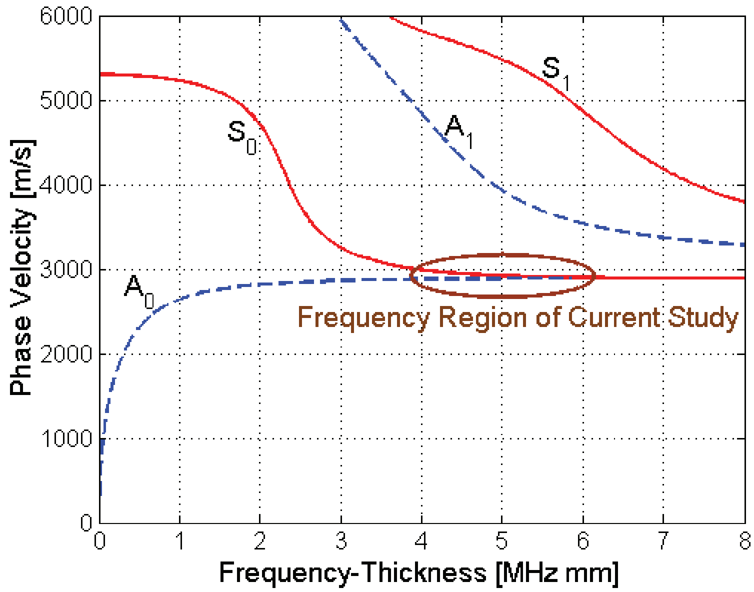


**FIGURE 1.** Phase velocity dispersion curves for steel plates showing guided ultrasonic wave modes and frequency-thickness range of interest for high frequency guided ultrasonic waves used in this study [20]. Reprinted with permission from AIP Conf. Proc. 1650, 777-784 (2015). Copyright 2015 American Institute of Physics.

Using a combination of time-of-flight and frequency evaluation of the reflected pulse, the defect location and damaged plate side could be determined [14]. Rayleigh-like waves were also used for in-situ monitoring of fatigue crack growth in tensile, aluminum specimens [19]. High frequency guided ultrasonic waves allow for the inspection of structures over reasonably long distances [20], and can be employed even if local access to the inspected part is not possible. Depending on the chosen frequency-thickness operating point, wavelengths are comparable to those used in bulk wave ultrasonic testing (UT), giving good sensitivity for small defect detection [12]. Continuing previously reported work for corrosion monitoring in steel structures [20], the superposition of the first anti-symmetric $A_0$ and symmetric $S_0$ Lamb wave modes at about 5 MHz mm (500 kHz excitation frequency in an approximately 10 mm thick steel plate) is investigated here [21]. These guided modes in plates can be selectively generated simultaneously using standard Rayleigh wave angle beam transducers and received using a laser interferometer. In this frequency range, there is a slight difference between the phase velocities of the first anti-symmetric ($A_0$) and symmetric ($S_0$) Lamb wave modes (Fig. 1). During wave propagation there is a continual shift in relative phase, causing the transfer of the wave energy through the plate thickness. This energy exchange happens over a distance, the so-called beatlength [22] or beat wavelength [23], given by

$$L = \frac{2\pi}{k_{A0} - k_{S0}}, \tag{1}$$

with $k_{A0}$ and $k_{S0}$ the wavenumbers of $A_0$ and $S_0$, respectively. This interference depends on the employed frequency thickness product, as it is governed by the inverse of the difference between the wave numbers of the two fundamental Lamb wave modes. This effect has been investigated in this study to monitor the thickness reduction due to generalized corrosion in steel specimens. The concept was in a first step visualized using 2D Finite Difference Method (FDM) simulations to predict the wave propagation phenomena. The 2D FDM modeling using a staggered grid and time marching algorithm is described. Following on from previously reported work to monitor the thickness reduction for milled, uniform thickness specimens and measurements for accelerated corrosion [2, 20], the applicability for non-uniform thickness reduction was investigated.

## 2D FINITE DIFFERENCE SIMULATION

The propagation of the two fundamental Lamb modes in the steel structure was predicted using a two-dimensional (2D) second-order, displacement-stress finite difference formulation. The equation of motion under small-deformation approximation and the stress-strain relations are discretized on a Cartesian, staggered grid for a two-dimensional, isotropic, linear elastic medium assuming plane strain wave propagation. This type of grid combines several types of nodes located at different positions and minimizes the number of variables per grid cell. The location of the displacement and stress components on the staggered grid is shown in Fig. 2. The boundary of the steel structure follows the shear stress nodes as illustrated in the upper part of Fig. 2. The stress-free boundary conditions at the material boundaries are imposed by assigning zero value to the corresponding shear stress nodes and adding a fictitious layer just outside the free surfaces for normal stress components and assigning specific values to the variables of the fictitious nodes to achieve zero normal stress at the material surface. As a general rule a minimum of 10 nodes per wavelength is required in order to reduce the numerical dispersion to an acceptable level [24]. For high-frequency guided waves, the mode shapes have to be approximated accurately and in general finer spatial sampling is required [25]. In this contribution, a grid size of 200 μm was selected in the direction of wave propagation, corresponding to a spatial sampling of 32 nodes per wavelength (approximately 6.5 mm at 450 kHz). The fundamental modes $A_0$ and $S_0$ were generated by imposing the whole displacement field in the two initial time steps of the time marching algorithm. The displacement components were computed at every node using FFT as described by Munasinghe [26]. The selected excitation signal was a sinusoidal, 10-cycle tone burst at a center frequency of 450 kHz.

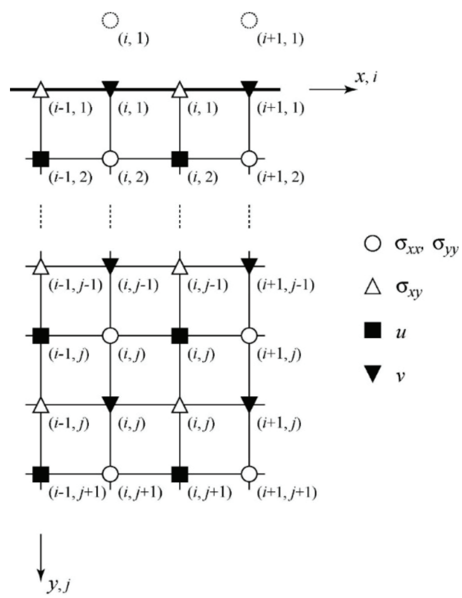


**FIGURE 2.** Staggered grid for 2D FDM simulations and illustration of the upper structure boundary with fictitious layer for normal stress component.

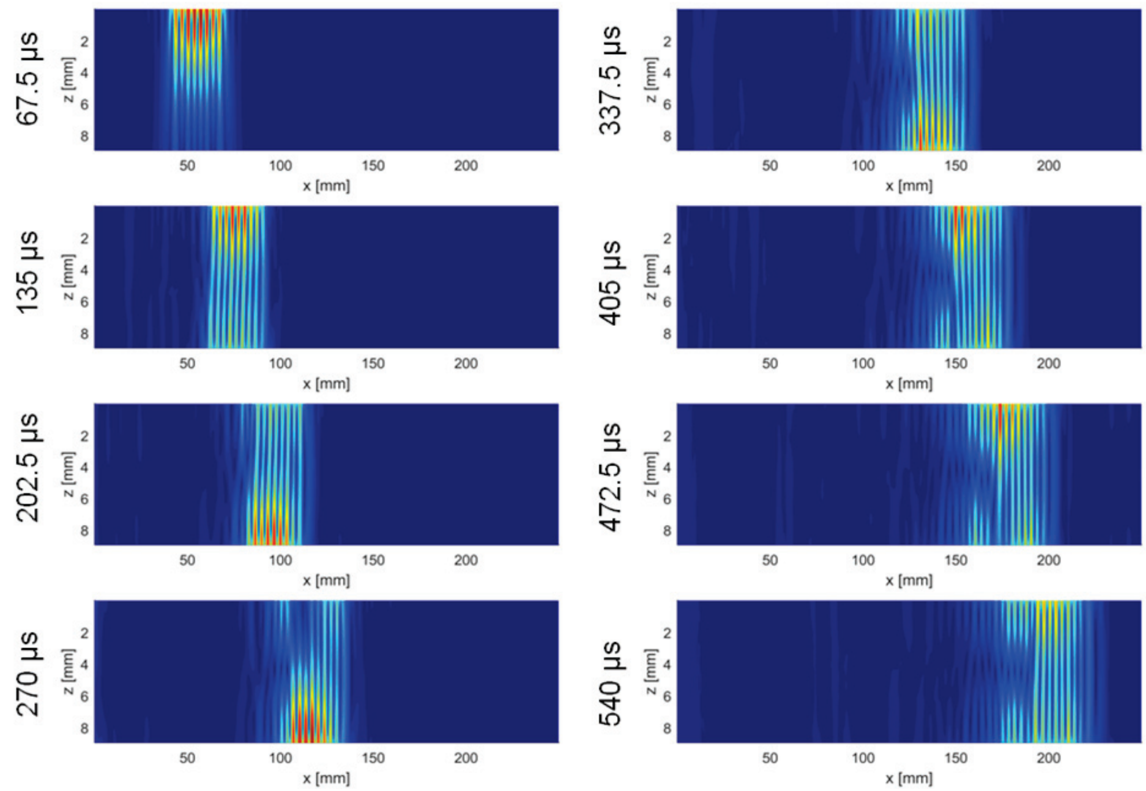


**FIGURE 3.** FDM simulation of wave propagation along 2D plate specimen at different time steps; excitation frequency 450 kHz; 10 cycles; 9 mm thick steel plate.

The 2D FDM model was employed to visualize the wave propagation along a 9 mm thick steel plate. The wave excitation was prescribed to simulate a transducer placed on the top surface ($A_0$ and $S_0$ in phase on the upper surface). For the different time snapshots shown in Fig. 3, it can be observed that as the wave pulse propagates along the plate, the distribution of the energy through the thickness changes. The initial snapshot (67.5 μs) shows most of the wave pulse energy located in the upper half of the plate thickness. Gradually more energy is transferred to the lower half of the plate thickness (270 μs), with reduced amplitude on the top surface and increased amplitude on the bottom surface. As the wave propagates farther, energy is transferred back to the upper half of the plate, with increased amplitude on the top surface (405 μs).

## EXPERIMENTS

Multiple plate specimens (600 mm x 100 mm) were cut from a single plate of mild steel (EN3B – AISI 1020) and then milled to 11 mm thickness in order to correct a slight curvature in the original plate material. The used mild steel is similar in mechanical properties to that of steel used in shipbuilding (Poisson's ratio 0.29, yield strength 295MPa, tensile strength 395MPa). One specimen was milled down in 0.2 mm steps to a final thickness of 9.6 mm to achieve a uniform thickness reduction [2]. Two specimens were subjected to accelerated corrosion to obtain generalized corrosion with a thickness reduction across the whole specimen area [27]. The setup consisted of a DC voltage source, the steel plate partially submerged as the anode in NaCl solution (salt water), suspended above the copper cathode [20]. The DC voltage source supplied a current of approximately 5A at 12V. The thickness was monitored using longitudinal pulse-echo ultrasonic measurements (5 MHz center frequency) at 6 different locations along the center line of the plate. The ultrasonic measurements were taken as the actual thickness values. Based on the predicted corrosion rates the accelerated corrosion was interrupted approximately every 44 hours to perform a guided ultrasonic wave measurement for thickness reductions matching approximately the 0.2 mm milling steps.

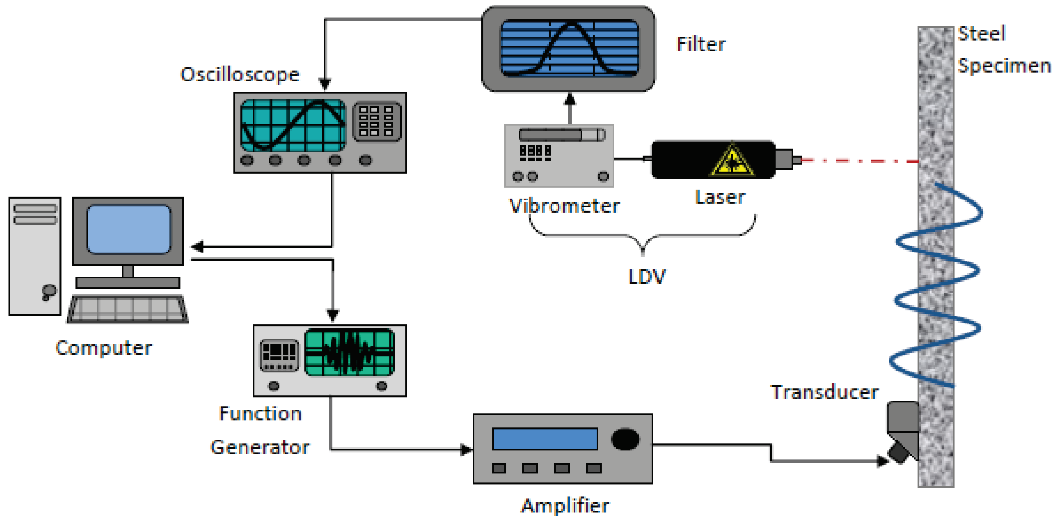


**FIGURE 4.** Experimental setup for laser measurement of high frequency guided ultrasonic wave propagation on steel specimen [20]. Reprinted with permission from AIP Conf. Proc. 1650, 777-784 (2015). Copyright 2015 American Institute of Physics.

The average thickness was in general close to the required thickness and reduced from 11.0 mm to 9.4 mm. The specimen surface showed the expected unevenness and roughness typical for the corrosion process. The high frequency guided ultrasonic waves ($A_0$ and $S_0$ modes) were generated at the upper plate surface using a standard Rayleigh angle beam transducer with a center frequency of 500 kHz. The wave propagation investigation was performed using a 10-cycle tone burst excitation (sinusoid in a Hanning window), generated in a programmable function generator and amplified using a broadband power amplifier. A heterodyne laser interferometer was used for point measurements of the velocity of the out-of-plane displacement field along the propagation of the ultrasonic pulse [28], as shown in Fig. 4. The interferometer head was moved parallel to the plate surface by means of a scanning rig with a step size of 1 mm for a distance of 450 mm from the transducer location. The signal was filtered using a band pass filter (400 – 600 kHz), averaged (50 averages) and recorded using a digital storage oscilloscope. Using Matlab the amplitude at a frequency of 450 kHz was extracted for each measurement location using Fast Fourier Transform (FFT). An evaluation frequency slightly below the center excitation frequency of 500 kHz was employed to achieve shorter beatlengths with multiple amplitude minima occurring over the measurement distance of 450 mm. Previous evaluations at 500 kHz had shown slight variations due to the fitting procedure of the observed amplitude values with limited propagation length relative to the beatlength.

## GUIDED WAVE PROPAGATION FOR UNIFORM THICKNESS REDUCTION

The first plate specimen was milled in 8 steps of 0.2 mm from a uniform thickness of 11.0 mm to a thickness of 9.6 mm. The second specimen was corroded as described above to a thickness of 9.4 mm. Periodically the specimen was taken out of the accelerated corrosion setup and the ultrasonic measurements conducted. The guided ultrasonic wave propagation along the center line of the specimen was measured and the amplitude at 450 kHz (FFT) versus propagation distance curve analyzed. The amplitude variation for the milled and corroded specimens at two thicknesses for each specimen is shown in Fig. 5. The amplitude decreases as the wave propagates from the excitation location and then periodically increases and decreases again [20]. For the thinner specimens a reduction in the beatlength, i.e. the maxima and minima occurring closer to each other, can be observed. The measured amplitude curves were fitted using Matlab with the theoretically predicted exponentially decreasing cosine curve. Good agreement for the principal features can be seen in Fig. 5 for the measurements at different plate thicknesses. The experimental beatlengths and the theoretically predicted values using equation (1) and Disperse [29] are shown in Fig. 6. Good general agreement and the reduction of beatlength with decreasing specimen thickness can be observed. An initial evaluation of the sensitivity of the methodology estimated a determination of the plate thickness reduction with a resolution of about 0.2 mm (2%), which would be more than sufficient to detect generalized corrosion before it affects the structural integrity of a ship hull or offshore installation.

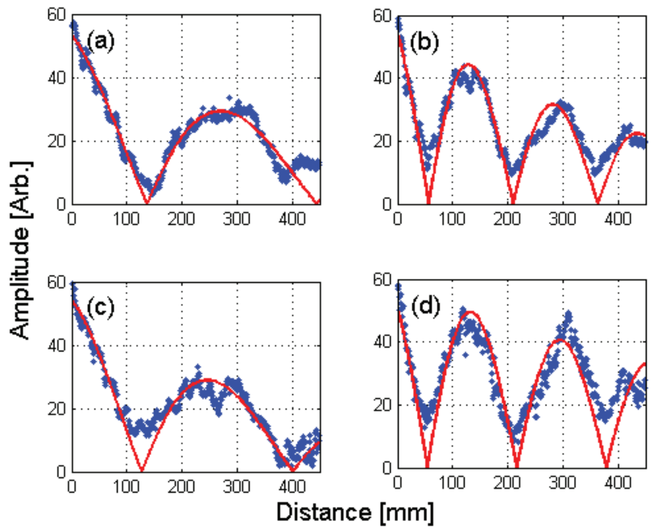


**FIGURE 5.** Measured amplitude of high frequency guided wave at 450 kHz (FFT) along milled and corroded steel specimens, measured using laser interferometer: a) 10.8 mm milled; b) 9.6 mm milled; c) 10.8 mm corroded; d) 9.4 mm corroded; measured amplitude: blue dots; exponential fit: red, solid line.

## GUIDED WAVE PROPAGATION IN TAPERED SPECIMEN

Corrosion often leads to varying thickness changes over the corroded surface. As a simple, controlled model for this, one steel specimen was milled to have a taper, with the thickness along the length (600 mm) changing linearly from 11 mm at one end to 8 mm at the other end. The wedge transducer was placed on the top surface at the thicker end and the high frequency guided wave propagation measured along both the top and bottom surfaces. The amplitude at 450 kHz was again extracted using FFT and is shown in Fig. 7. Comparing the amplitudes on the top and bottom surfaces, the energy exchange through the specimen thickness can be observed.

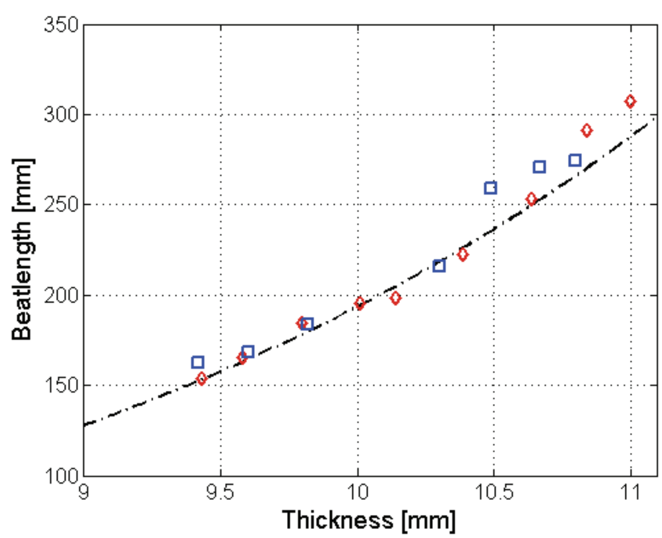


**FIGURE 6.** Comparison of theoretically predicted beatlength at 450 kHz versus plate thickness (dash-dotted, black line) against measured beatlength (fit from laser amplitude measurements at 450 kHz); milled specimen: red diamonds; corroded specimen: blue squares.

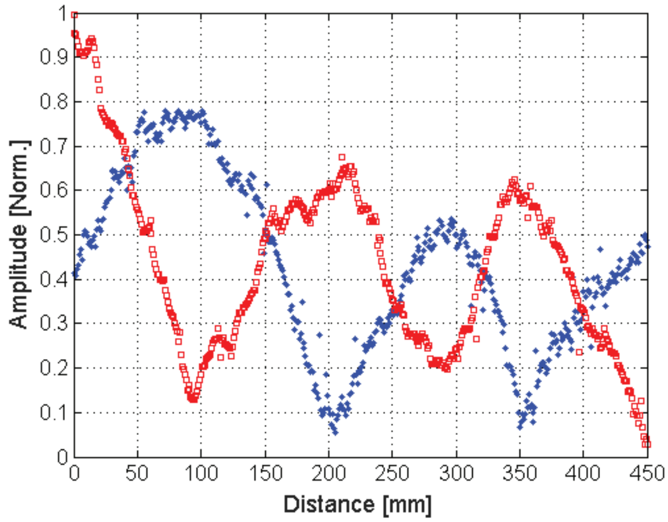


**FIGURE 7.** Measured amplitude of high frequency guided wave at 450 kHz (FFT) along milled steel specimen with linearly varying thickness (11 to 8 mm), measured using laser interferometer; front (transducer) side: red squares, back side: blue dots.

The first minimum of the amplitude on the top surface at about 100 mm corresponds to the maximum amplitude on the bottom surface, and the minimum of the amplitude on the back surface at approximately 200 mm corresponds to high amplitude at the top surface. Looking at the amplitude pattern and especially the distance at which the minima occur (e.g. about 100 and 280 mm on top surface, 200 and 350 mm on bottom surface), it is possible to observe the expected reduction in beatlength with plate thickness (11 mm to 8 mm) along the wave propagation distance. Due to the gradual change in thickness (0.5 mm per 100 mm) no reflections were observed and the time traces (not shown) did not show a different pattern as compared to the constant thickness measurements. Further investigations will compare the experimental measurements to predictions using the 2D FDM simulations and look at more complex changes in thickness.

## CONCLUSIONS

Wall thickness loss is a significant problem for marine structures exposed to corrosive environments, including ship hulls and offshore installations. High frequency guided ultrasonic waves can propagate along the structure and permit nondestructive measurements over reasonable propagation lengths. The measurement setup was simulated using a 2D FDM scheme and the expected wave propagation and mode interference visualized. High frequency guided wave modes at about 5 MHz mm frequency thickness product (500 kHz in approximately 10 mm thick steel plate) were excited using a standard wedge transducer and measured using a laser interferometer. With good accuracy the two fundamental Lamb modes ($A_0$ and $S_0$) were selectively excited simultaneously. Their interference pattern over a length scale called the beatlength is very sensitive to changes in the plate thickness as it depends on the inverse of the difference in the respective wavenumbers. Uniform plate thickness reduction was achieved by milling one plate specimen to the required thickness and accelerated corrosion was employed to reduce the wall thickness of another specimen. This resulted in some unevenness and roughness of the plate surface due to the corrosion process. The amplitude beatlength was quantified from a fit of the experimentally measured amplitude curves along the propagation distance and good agreement of the measured beatlengths with theoretical predictions was achieved. This demonstrated the sensitivity of the proposed methodology down to about 2% wall thickness loss under laboratory conditions. Initial experiments were conducted for a milled, tapered specimen to investigate the sensitivity of the high frequency guided ultrasonic waves to varying thickness profiles along the propagation path. Further studies should explore this for more realistic thickness variations and compare experimental results to numerical simulation predictions.

## ACKNOWLEDGMENTS

The authors would like to thank Daniel Chew for his contribution to the corrosion measurements and the UCL Mechanical Engineering workshop for the precision machining.

## REFERENCES


1. T. Nakai, H. Matsushita, N. Yamamoto, and H. Arai, *Marine Struct.* **17**, 403-432 (2004).
2. D. Chew and P. Fromme, "Monitoring of corrosion damage using high-frequency guided ultrasonic waves," *Proc. SPIE*, **9064**, 90642F (2014).
3. P. Fromme, P. D. Wilcox, M.J.S. Lowe, and P. Cawley, *IEEE Trans. Ultrason. Ferroelectr. Freq. Control* **53**, 777-785 (2006).
4. J.S. Hall, P. Fromme, and J.E. Michaels, *J. Nondestruct. Eval.* **33**, 299-308 (2014).
5. P. Fromme, "Health Monitoring of Plate Structures using Guided Waves," *Proc. SPIE* **6935**, 69350W (2008).
6. J. L.Rose, *Mat. Eval.* **60**, 53-59 (2002).
7. Z. Fan, M. Castaings, M.J.S. Lowe, C. Biateau, and P. Fromme, *NDT&E Int.* **54**, 96-102 (2013).
8. D. N. Alleyne, and P. Cawley, *IEEE Trans. Ultrason. Ferroelectr. Freq. Control* **39**, 381-397 (1992).
9. P. Fromme, P.D. Wilcox, M. Lowe, and P. Cawley, "On the Scattering and Mode Conversion of the $A_0$ Lamb Wave Mode at Circular Defects in Plates," in *Review of Progress in Quantitative Nondestructive Evaluation*, eds. D.O. Thompson and D.E. Chimenti, American Institute of Physics 700, Melville, NY) **23**, 142-149 (2004).
10. P. Fromme, "Monitoring of Plate Structures Using Guided Ultrasonic Waves," in *Review of Progress in Quantitative Nondestructive Evaluation*, eds. D.O. Thompson and D.E. Chimenti, (American Institute of Physics 975, Melville, NY) **27**, 78-85 (2008).
11. N. Terrien, D. Osmont, D. Royer, F. Lepoutre, and A. Déom, *Ultrasonics* **46**, 47-78 (2007).
12. D.W. Greve, P. Zheng, and I.J. Oppenheim, *Smart Mater. Struct.* **17**, 035029 (2008).
13. D. Ratnam, K. Balasubramaniam, and B.W. Maxfield, *IEEE Trans. Ultrason. Ferroelectr. Freq. Control* **59**, 727-737 (2012).
14. B. Masserey and P. Fromme, *J. Acoust. Soc. Am.* **123**, 88-98 (2008).
15. B. Masserey and P. Fromme, *NDT&E Int.* **42**, 564-572 (2009).
16. B. Masserey and P. Fromme, *NDT&E Int.* **71**, 1-7 (2015).
17. H. Chan, B. Masserey, and P. Fromme, *Smart Mater. Struct.* **24**, 025037 (2015).
18. B. Masserey, C. Raemy, and P. Fromme, *Ultrasonics* **54**, 1720-1728 (2014).
19. B. Masserey and P. Fromme, *Struct. Health Monit.* **12**, 484-493 (2013).
20. D. Chew and P. Fromme, "High-frequency Guided Waves for Corrosion Monitoring," in *Review of Progress in Quantitative Nondestructive Evaluation*, eds. D.E. Chimenti, L.J. Bond, and D.O. Thompson, (American Institute of Physics 1650, New York, **34**, 777-784 (2015).
21. I. A. Viktorov, *Rayleigh and Lamb Waves*, (Plenum Press, NY) pp. 93-96 (1967).
22. B. W. Ti, W. D. O'Brien, and J. G.Harris, *J. Acoust. Soc. Am.* **102**, 1528-1531 (1997).
23. B.A. Auld, *Acoustic Fields and Waves in Solids*, New York, Wiley, **2**, 93-94 (1973).
24 J. Virieux, *Geophysics* **51**, 889–901 (1986).
25 B. Masserey and E. Mazza, *J. Acoust. Soc. Am.* **118**, 3585–3594 (2005).
26 M. Munasinghe and G. W. Farnell, *J. Geophys. Res.* **78**, 2454-2466 (1973).
27. F. Cegla, P. Cawley, J. Allin, and J. Davies, *IEEE Trans. Ultrason. Ferroelectr. Freq. Control* **58**, 156-167 (2011).
28. P. Fromme and M. B. Sayir, *Ultrasonics* **40**, 199-203 (2002).
29. B. Pavlakovic, M. J. S. Lowe, D. Alleyne, and P. Cawley, "Disperse: A General Purpose Program for Creating Dispersion Curves," in *Review of Progress in Quantitative Nondestructive Evaluation*, eds. D.O. Thompson and D.E. Chimenti, (Plenum Press, NY) **16**, 185-192 (1997).